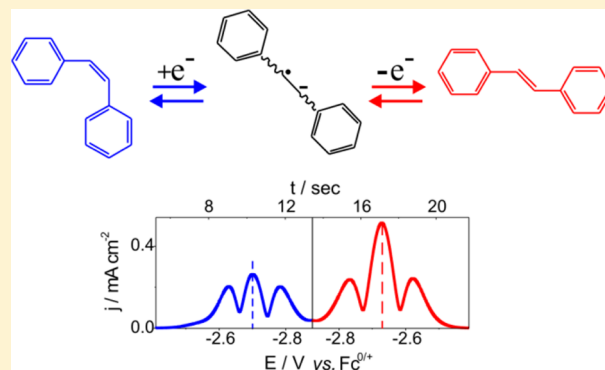


Studies on the Nuances of the Electrochemically Induced Room Temperature Isomerization of *cis*-Stilbene in Acetonitrile and Ionic LiquidsOmar Abdul-Rahim,<sup>†,||</sup> Alexandr N. Simonov,<sup>\*,†</sup> John F. Boas,<sup>‡</sup> Thomas R  ther,<sup>§</sup> David J. Collins,<sup>†</sup> Patrick Perlmutter,<sup>†</sup> and Alan M. Bond<sup>\*,†</sup><sup>†</sup>School of Chemistry, Monash University, Clayton, Victoria, 3800, Australia<sup>‡</sup>School of Physics, Monash University, Clayton, Victoria, 3800, Australia<sup>§</sup>CSIRO Energy Transformed Flagship, Clayton, Victoria, 3168, Australia

## S Supporting Information

**ABSTRACT:** Electrochemical reduction of *cis*-stilbene occurs by two well-resolved one-electron reduction steps in acetonitrile with (*n*-Bu)<sub>4</sub>NPF<sub>6</sub> as the supporting electrolyte and in *N*-butyl-*N*-methylpyrrolidinium (Pyr<sub>1,4</sub><sup>+</sup>) and (trimethylamine)-(dimethylethylamine)-dihydroborate bis(trifluoromethylsulfonyl)-amide (NTf<sub>2</sub><sup>-</sup>) ionic liquids (ILs). Mechanistic details of the electroreduction have been probed by dc and Fourier transformed ac voltammetry, simulation of the voltammetry, bulk electrolysis, and EPR spectroscopy. The first one-electron reduction induces fast *cis* to *trans* isomerization in CH<sub>3</sub>CN and ILs, most likely occurring via disproportionation of *cis*-stilbene radical anions and fast transformation of the *cis*-dianion to the *trans*-configuration. The second reduction process is chemically irreversible in CH<sub>3</sub>CN due to protonation of the dianion but chemically reversible in highly aprotic ILs under high *cis*-stilbene concentration conditions. Increase of the (*n*-Bu)<sub>4</sub>NPF<sub>6</sub> supporting electrolyte concentration (0.01–1.0 M) in CH<sub>3</sub>CN induces substantial positive shifts in the potentials for reduction of *cis*-stilbene, consistent with strong ion pairing of the anion radical and dianion with (*n*-Bu)<sub>4</sub>N<sup>+</sup>. However, protection by ion pairing against protonation of the stilbene dianions or electrochemically induced *cis*–*trans*-stilbene isomerization is not achieved. Differences in electrode kinetics and reversible potentials for *cis*-stilbene<sup>0/•-</sup> and *trans*-stilbene<sup>0/•-</sup> processes are less pronounced in the Pyr<sub>1,4</sub>–NTf<sub>2</sub> ionic liquid than in the molecular solvent acetonitrile.

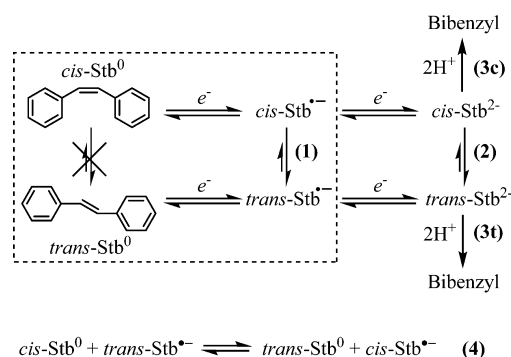


## ■ INTRODUCTION

Examples of isomerization induced by electrochemical reduction or oxidation include *cis/trans* and *fac/mer* rearrangements with coordination compounds<sup>1</sup> as well as *E/Z* transformations of conjugated olefins.<sup>2–5</sup> In many cases, isomerization occurs immediately after charge transfer via the so-called EC mechanism (where E stands for an electrochemical step and C stands for a homogeneous chemical reaction). An early example of a rearrangement of *cis*-stilbene (*cis*-Stb) to *trans*-stilbene (*trans*-Stb) induced by one-electron reduction of the *cis*-isomer<sup>6,7</sup> was initially regarded as an EC case (dashed box in Scheme 1) complicated by the cross redox reaction between the radical anions (*cis*- and *trans*-Stb<sup>•-</sup>) and neutral stilbene molecules (reaction 4 in Scheme 1).<sup>8,9</sup> However, later reports (*vide infra*) suggest that the mechanism for reduction of *cis*-Stb is even more complicated.

Initial attempts to distinguish between the radical anions produced as a result of one-electron reduction of *cis*- and *trans*-stilbenes used electron paramagnetic resonance (EPR), UV–vis, and Raman spectroscopy. However, in these studies,

Scheme 1. Reaction Scheme for Electrochemically Induced *cis/trans* Isomerization of Stilbene

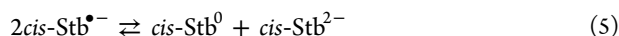


Received: January 22, 2014

Revised: February 18, 2014

Published: February 21, 2014

detection of the same radical anion with an assumed *trans*-configuration was always reported.<sup>8–12</sup> The first indirect evidence that indicated a significant difference between the *cis*- and *trans*-anion radicals was acquired from characterization of the products of their interaction with CO<sub>2</sub><sup>13</sup> and kinetic analyses of the isomerization of *cis*- to *trans*-stilbene that accompanied chemical reduction.<sup>12,14</sup> Spectroscopic proof of the distinction between the *cis*- and *trans*-Stb<sup>•−</sup> radical anions was finally obtained with the aid of pulse radiolysis and flash photolysis techniques,<sup>15–17</sup> as well as by EPR analysis of *cis*-Stb<sup>•−</sup> at low temperatures in the presence of unreduced *cis*-Stb.<sup>18,19</sup> The influence of neutral *cis*-Stb<sup>0</sup> on the stability of the *cis*-radical anion was proposed to arise from the suppression of the disproportionation reaction 5.



As suggested by Szwarc and co-workers<sup>12,17,18,20</sup> and further underpinned by low-temperature EPR kinetics<sup>19</sup> and dc cyclic voltammetric studies,<sup>2</sup> direct *cis*-Stb<sup>•−</sup> → *trans*-Stb<sup>•−</sup> isomerization (reaction 1, Scheme 1) is slow, at least at low temperatures, and it was proposed that the dominant route for isomerization of the *cis*-Stb<sup>•−</sup> anion radical is via reaction 5 and subsequent fast transformation of *cis*-Stb<sup>2−</sup> to *trans*-Stb<sup>2−</sup> (reaction 2, Scheme 1).

The extremely high rate of isomerization of *cis*-Stb<sup>2−</sup> to *trans*-Stb<sup>2−</sup>, even at low temperatures, makes it difficult to obtain unambiguous experimental proof of the dissimilarity of the dianions. However, *cis*- and *trans*-Stb<sup>2−</sup> were claimed by Szwarc and co-workers to be different species on the basis of analysis of kinetic data obtained under conditions favoring association of the stilbene dianions with alkali metal cations.<sup>20</sup> In a later paper, Szwarc et al.<sup>17</sup> showed that the dianions formed during chemical reduction of *cis*- and *trans*-stilbene are indistinguishable when interaction between Stb<sup>2−</sup> and cations is suppressed. The importance of reaction 5 and the strength of interaction between the stilbene dianions and cations in the mechanism of the *cis/trans*-Stb isomerization was also emphasized by Combella et al.<sup>2</sup> on the basis of detailed dc voltammetric analysis of the reduction of *cis*-Stb in liquid ammonia at 235 K.

The only study on the room temperature electrochemical reduction of *cis*-Stb published to date is a qualitative report by Bard et al.,<sup>8</sup> who reported the transformation of the *cis*-radical anion to the *trans*-isomer upon one-electron electroreduction in *N,N*-dimethylformamide. In the present paper, an examination of the nuances of electroreduction of *cis*-Stb at ca. 298 K has been undertaken by the mechanistically sensitive technique of Fourier transformed ac (FTAC) voltammetry<sup>21</sup> in conjunction with classic dc voltammetry and bulk electrolysis in the molecular solvent acetonitrile containing tetrabutylammonium hexafluorophosphate ((*n*-Bu)<sub>4</sub>NPF<sub>6</sub>) as the supporting electrolyte. Cyclic voltammetric studies are also reported in the highly aprotic *N*-butyl-*N*-methylpyrrolidinium (Pyr<sub>4,1</sub><sup>+</sup>) and (trimethylamine)(dimethylethylamine)-dihydroborate ((N<sub>111</sub>)-(N<sub>112</sub>)BH<sub>2</sub><sup>+</sup>) bis(trifluoromethylsulfonyl)-amide (NTf<sub>2</sub><sup>−</sup>) based ionic liquids (ILs) which have very recently been shown to be highly suitable media for the stabilization of stilbene dianions on the voltammetric time scale at room temperature.<sup>22</sup> Although of limited use because of difficulty of obtaining a unique solution with a multitude of unknown parameters, simulations based on different scenarios for the electrochemically induced *cis/trans* isomerization of stilbene at room temperature are compared with experimental data. Results are compared to those available on the reduction of *trans*-Stb to its

radical anion and dianion.<sup>22</sup> A brief report on electrochemical reduction of *cis*-4-methoxystilbene also is provided.

## EXPERIMENTAL SECTION

**Materials.** Acetonitrile (Lichrosolv HPLC grade; Merck) was distilled over calcium hydride, transferred using a cannula into a sealed flask, and immediately introduced into a glovebox. All of these operations were performed under a high purity nitrogen atmosphere (99.999%, H<sub>2</sub>O < 3 ppm, O<sub>2</sub> < 2 ppm). (*n*-Bu)<sub>4</sub>NPF<sub>6</sub> (98%, Wako or Beijing Health Science and Technology Co.) was recrystallized twice from ethanol (96%, Merck Emplura) and dried under a vacuum at 313 K for at least 24 h prior to use. The ultrapure Pyr<sub>4,1</sub>-NTf<sub>2</sub> IL (>99%; bottled under Ar; Merck Millipore) and CD<sub>3</sub>CN (≥99.98%; Merck Magnisolv, for NMR spectroscopy) were unpacked inside the glovebox and used as received. The (N<sub>111</sub>)(N<sub>112</sub>)-BH<sub>2</sub>-NTf<sub>2</sub> IL (95%, Frontier Scientific) was purified as described elsewhere.<sup>22</sup> *Trans*-Stilbene (*t*-Stb; 96%, Sigma-Aldrich), *cis*-stilbene (96%, Sigma-Aldrich), *cis*-4-methoxystilbene (>95%, Sigma-Aldrich), ferrocene (Fc; 98%, Riedel-deHaen), and AgNO<sub>3</sub> (99.998%, Sigma-Aldrich) were used as received.

### Electrochemical Instrumentation and Procedures.

Electrochemical experiments were performed in three-electrode cells at 296–300 K under glovebox conditions using either an Epsilon Electrochemical Workstation (BAS) or a homemade FTACV instrument.<sup>21</sup> The working electrodes were glassy carbon (GC, diameter 1 or 3 mm) and Au (diameter 2 mm) macrodisks or a carbon fiber microelectrode (diameter 12 μm) pretreated using standard procedures, which are detailed in the Supporting Information. During and between experiments, a high purity dry N<sub>2</sub> atmosphere was maintained continuously inside the glovebox. Potentials are reported versus the formal potential of the Fc<sup>0/+</sup> couple, as measured in the same solution and precisely determined by simulation. Unless otherwise stated, current data are normalized to the electrode surface area.

**EPR Spectroscopy.** Reductive bulk electrolysis of *cis*-stilbene in CH<sub>3</sub>CN (0.1 M (*n*-Bu)<sub>4</sub>NPF<sub>6</sub>) under glovebox conditions was undertaken at ambient temperature (~296–298 K) to generate the anion radical. EPR spectra were obtained from these solutions at 120 and 250 K with a Bruker ESP380E CW/FT X-band (ca. 9.4 GHz) spectrometer as described in the Supporting Information.

**Theory.** Simulations of the dc and ac voltammograms are based on a Butler–Volmer model for electron transfer with all charge transfer (α) values fixed at 0.50 and were undertaken using DigiElch – Professional 7.F<sup>23</sup> and Monash Electrochemistry Simulator (MECSim) software packages,<sup>24</sup> respectively.

## RESULTS AND DISCUSSION

**Stability of *cis*-Stilbene in CH<sub>3</sub>CN.** Thermodynamically, *trans*-Stb is greatly favored over the *cis*-isomer. Thus, it is essential to confirm that no *cis* → *trans* isomerization occurs prior to undertaking voltammetric experiments. In acetonitrile in the absence and in the presence of the supporting electrolyte, the stability of *cis*-Stb initially was assessed by <sup>1</sup>H NMR spectroscopy. <sup>1</sup>H NMR spectra of the freshly prepared 4 mM *cis*-Stb solutions in neat CD<sub>3</sub>CN exhibited signals corresponding exclusively to the *cis*-isomer with no evidence of the presence of the *trans*-counterpart. Analogous <sup>1</sup>H NMR results were obtained for a *cis*-Stb solution in CD<sub>3</sub>CN containing 0.1

M (*n*-Bu)<sub>4</sub>NPF<sub>6</sub>, which was used as the electrolyte in the voltammetric studies. Thus, voltammetric studies can be undertaken on pure (NMR perspective) *cis*-Stb. Cyclic voltammograms for reduction of *cis*-Stb (Figure 1) do not

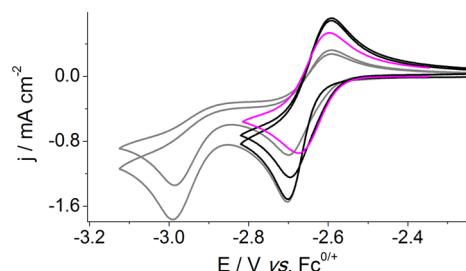


**Figure 1.** dc cyclic voltammograms ( $\nu = 0.10 \text{ V s}^{-1}$ ) for reduction of 3.1 mM *cis*-stilbene (black and gray, the first two cycles of potential are shown) and 2.3 mM *trans*-stilbene (magenta) with a GC electrode in CH<sub>3</sub>CN (0.1 M (*n*-Bu)<sub>4</sub>NPF<sub>6</sub>).

change when recorded uninterruptedly for 10 min without any precautions being taken to exclude impact of light, noting that photoisomerization of *cis*- to *trans*-Stb has been reported in other electrochemical studies.<sup>8</sup> Finally, negligible differences were found between the dc voltammograms obtained with a GC electrode for reduction of *cis*-Stb in CH<sub>3</sub>CN (0.1 M (*n*-Bu)<sub>4</sub>NPF<sub>6</sub>) immediately and 48 h after preparation of the solution. Thus, it was found that *cis*-Stb solutions in acetonitrile are sufficiently stable for undertaking room-temperature electrochemical studies and, furthermore, the use of relatively low surface area macrodisk electrodes does not initiate detectable changes in the composition of the bulk solution.

**Steady State Voltammetry of *cis*-Stilbene in CH<sub>3</sub>CN.** In accordance with expectations based on the mechanism given in Scheme 1 and related ones, near steady-state microdisk voltammograms obtained for reduction of *cis*-Stb in dry acetonitrile with (*n*-Bu)<sub>4</sub>NPF<sub>6</sub> supporting electrolyte (Figure S1, Supporting Information) consist of two consecutive electron-transfer events that are qualitatively similar to the RDE data reported previously for the *trans*-isomer.<sup>22</sup> That is, similar limiting current magnitudes ( $I_{\text{DL}}$ ) are found for each process, as expected if both are one-electron reductions. However,  $I_{\text{DL}}$  for the first reduction step is always greater than that for the second process, suggesting a contribution from homogeneous chemical processes occurs after the initial step in the reduction of *cis*-Stb.

**dc Cyclic Voltammetry of *cis*-stilbene and *cis*-4-Methoxystilbene in CH<sub>3</sub>CN.** Analysis of dc cyclic voltammograms for the reduction of *cis*-Stb at a GC macrodisk electrode in CH<sub>3</sub>CN (0.1 M (*n*-Bu)<sub>4</sub>NPF<sub>6</sub>) reveals that fundamental differences exist compared to the reduction of *trans*-Stb (Figure 1).

The peak current ( $I_{\text{p}}^{\text{Red}}$ ) in the first cycle of potential for reduction of *cis*-Stb (black curves in Figure 1) in CH<sub>3</sub>CN (0.1 M (*n*-Bu)<sub>4</sub>NPF<sub>6</sub>) exhibits a close to linear dependence on concentration (1–5 mM) and the square root of the scan rate ( $\nu = 0.10$ – $1.0 \text{ V s}^{-1}$ ) (Figure S2, Supporting Information) as also in the case for the reduction of *trans*-Stb.<sup>22</sup> However, the peak potential for reduction of *cis*-Stb is always more negative than that for the *trans*-counterpart by about 0.03 V over the concentration range 1–5 mM and scan rate 0.10– $1.0 \text{ V s}^{-1}$ . In contrast, the potentials for the second reduction steps are essentially indistinguishable. Furthermore, the peak-to-peak

separation ( $\Delta E_{\text{p}}$ ) in the first cycle is substantially larger than the value expected for a reversible one-electron transfer process, and larger than that found for the *trans*-Stb<sup>0/•−</sup> process (Table S1, Supporting Information), which mimics values found for the reversible Fc<sup>0/+</sup> process ( $I_{\text{R}}$  drop gives rise to a small departure from fully ideal reversible behavior in both *trans*-Stb<sup>0/•−</sup> and Fc<sup>0/+</sup> cases). Evolution of the dc voltammetry in the acetonitrile solutions of *cis*-Stb on multiple cycling of the potential (Figure 1) closely resembles that reported for the low-temperature electroreduction of this isomer in liquid ammonia in the presence of Mg<sup>2+</sup> cations.<sup>2</sup> In particular, a pronounced increase of reductive current in the second and subsequent cycles commences at more positive potentials than in the first cycle and a shoulder emerges that coincides in potential with that found in cyclic voltammetric reduction of *trans*-Stb (Figure 1). These data imply isomerization of *cis*-Stb<sup>•−</sup> to *trans*-Stb<sup>•−</sup> occurs on the dc voltammetric time scale at room temperature. dc Voltammetric behavior for the initial one-electron reduction of *cis*-Stb is essentially identical at GC and Au electrodes. However, the potential for the second irreversible reduction step is ca. 0.08 V more negative at the gold surface (Figure S3, Supporting Information). Other characteristics associated with the second irreversible reduction steps are similar at both electrode surfaces.

Introduction of a methoxy substituent into the *para* position of *cis*-stilbene does not cause major changes in the profile of the dc voltammetric reduction (Figure S3b, Supporting Information), which probably occurs via the same mechanism. However, in accordance with the increase of the electron density in the stilbene molecule due to interplay of induction and resonance effects resulting from substitution of the *para*-proton with the CH<sub>3</sub>–O– group,<sup>25</sup> the dc voltammetric curves obtained for reduction of *cis*-4-methoxystilbene are shifted by ca. 0.13 V to more negative potentials as compared with the unsubstituted *cis*-Stb.

**ac Cyclic Voltammetry of *cis*-Stilbene in CH<sub>3</sub>CN.** Examination of the higher order harmonic components of the first cycle of ac voltammograms for the first *cis*-Stb reduction process in acetonitrile provides cogent evidence that different species are responsible for the well-defined responses in the reductive (negative potential scan direction) and oxidative (positive potential scan direction) sweeps (black curve in Figure 2). Significantly, the peak potentials and shapes of the higher harmonic components detected in the reverse scan (positive potential sweep) are in complete agreement with those obtained following reduction of *trans*-Stb under similar conditions (cf. black and magenta data in right panels of Figure 2). In this context, FTAC voltammetry confirms that fast isomerization of *cis*-Stb<sup>•−</sup> to *trans*-Stb<sup>•−</sup> occurs. The second cycle of potential also provides direct access to an accurate value of the formal standard potential of the *trans*-Stb<sup>0/•−</sup> process, unlike the dc voltammetric technique, where resolution is relatively poor. The harmonic components derived from the second cycle in the negative potential scan regime in FTAC voltammetry for the initial one-electron process result from overlapping *cis*-Stb<sup>0/•−</sup> and *trans*-Stb<sup>0/•−</sup> processes, while the second cycle reverse (positive potential) sweep is virtually identical to that found in the first (cf. green and black data in Figure 2) and subsequent cycles.

A lower current magnitude in the higher harmonic components per unit concentration for reduction of *cis*-Stb as compared to reduction of the *trans*-isomer (Figure 2) implies that the electrode kinetics for the *cis*-Stb<sup>0/•−</sup> process differs



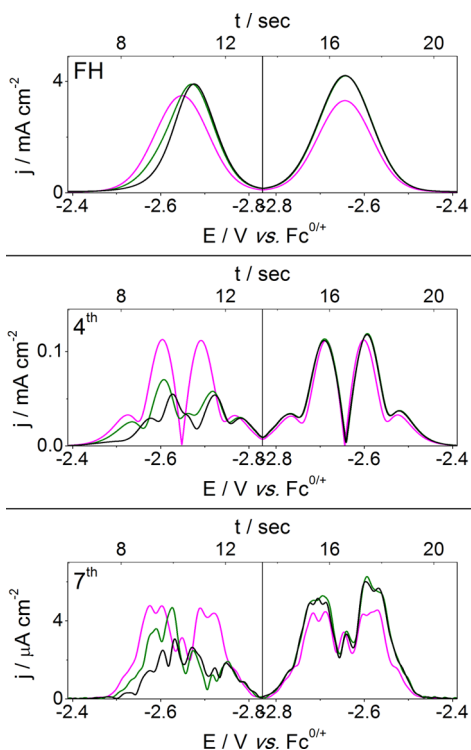


**Figure 2.** Fundamental, fourth and seventh ac harmonic components of FTAC cyclic voltammograms obtained for reduction of 3.1 mM *cis*-stilbene during the first two cycles of dc potential (black, first; green, second) and 2.3 mM *trans*-stilbene (magenta) in CH<sub>3</sub>CN (0.1 M (*n*-Bu)<sub>4</sub>NPF<sub>6</sub>) with a Au electrode.  $f = 9$  Hz,  $\Delta E = 0.08$  V,  $\nu = 0.060$  V s<sup>-1</sup>. The time scale refers to the black data.

substantially from that of the *trans*-Stb<sup>0/•-</sup> one. This could be a result of a lower heterogeneous electron transfer rate constant ( $k^0$ ), a contribution from the homogeneous reaction associated with *cis* to *trans* isomerization, or a combination of both.

**Reductive Bulk Electrolysis of *cis*-Stilbene in CH<sub>3</sub>CN and EPR Spectroscopic Characterization of the Anion Radicals.** If *cis*–*trans* isomerization occurs under short time cyclic voltammetric conditions, it should be far more substantial in longer time scale bulk electrolysis experiments. Reductive bulk electrolysis of *cis*-Stb at a Pt-gauze electrode at a constant potential of  $-2.79$  V at 296–298 K should generate *cis*- or *trans*-stilbene radical anions or a mixture of both. Initially, the solution developed a purple color followed by a change to black-brown with longer electrolysis times. On removal of the potential, the color rapidly faded and became pale yellow in ca. 10 min, demonstrating the limited stability of the radical anion species. The relatively short lifetime (minutes) of the Stb<sup>•-</sup> species was also confirmed by coulometric data. During exhaustive oxidative electrolysis at  $-2.20$  V of the stilbene anion radicals, the charge associated with oxidation of Stb<sup>•-</sup> never exceeded 20% of the charge required for reduction of neutral stilbene.

dc Cyclic voltammograms derived from partially reduced (50–60 mol %) solutions of *cis*-Stb revealed the classic characteristics expected for a diffusion-controlled one-electron process with the midpoint potential ( $E_m$ ) identical to that found for the *trans*-Stb<sup>0/•-</sup> process. FTAC voltammetric analysis of the electrolyzed acetonitrile solutions derived from bulk reduction of *cis*-Stb as well as of those subsequently subjected to bulk oxidative electrolysis unequivocally showed

that these electrolyzed solutions are dominated by species capable of fast and reversible electron transfer, uncomplicated by coupled chemical transformations (Figure S4, Supporting Information). This species is most likely to be the *trans*-Stb<sup>0</sup> form generated by electrolysis. In support of this hypothesis, deliberate addition of *trans*-stilbene was noted to simply enhance the *trans*-Stb<sup>0/•-</sup> process (Figure S4, Supporting Information). Finally, both low- (9 Hz) and high-frequency (219 Hz) experimental FTACV data are well fitted by the simulated curves on the basis of use of  $k^0$  and  $E^0$  values determined independently for the *trans*-Stb<sup>0/•-</sup> process using solutions of pure *trans*-Stb with GC ( $k^0 = 1.5$  cm s<sup>-1</sup>)<sup>22</sup> or Au ( $k^0 = 0.2$  cm s<sup>-1</sup>; Figure S4, Supporting Information) electrodes under similar conditions.

The presence of neutral *trans*-Stb<sup>0</sup> and the absence of *cis*-Stb<sup>0</sup> could be voltammetrically demonstrated after partial reductive bulk electrolysis. High resolution EPR spectroscopy should in principle provide a means of identifying the isomeric form of radical anions produced by reduction of *cis*-Stb. On the basis of the low-temperature study (183 K), Gerson et al.<sup>18</sup> reported that the center of the spectrum of *cis*-Stb<sup>•-</sup> is shifted to higher field by 0.008 mT relative to that of *trans*-Stb<sup>•-</sup> at 320 mT. This translates to a decrease in *g*-value of around 0.000 05 for the *cis*-Stb<sup>•-</sup> relative to that of *trans*-Stb<sup>•-</sup>. Furthermore, simulations of the EPR spectra of liquid phase solutions of *cis*-Stb<sup>•-</sup> and *trans*-Stb<sup>•-</sup>, using the proton hyperfine coupling constants reported by, e.g., Gerson et al.<sup>18</sup> and Nozaki et al.,<sup>19</sup> show that the overall widths of the spectra are around 2.70 and 2.90 mT, respectively.

The EPR spectrum obtained at 120 K after a *cis*-Stb solution was electrolyzed for 23–25 min at  $-2.79$  V at a Pt gauze electrode and rapidly frozen in liquid nitrogen was indistinguishable within experimental uncertainties from that of the *trans*-Stb<sup>•-</sup> radical anion generated by reduction of *trans*-Stb described elsewhere (Figure S5 and Table S2, Supporting Information).<sup>22</sup> The liquid phase EPR spectrum at 250 K derived from a *cis*-Stb solution in CH<sub>3</sub>CN, after reductive electrolysis, consisted of around 100 resonances centered at  $g = 2.002\,78 \pm 0.000\,02$  and extended over a field range of at least 2.7 mT (Figure S5 and Table S2, Supporting Information). This EPR spectrum was a factor of around 5 times less intense than that of *trans*-Stb solutions acquired previously under close to the same electrolysis conditions and EPR instrumental settings.<sup>22</sup> The difference in *g*-values between the spectra of the radical observed here for the electroreduced *cis*-Stb solution and that of the *trans*-Stb<sup>•-</sup> radical<sup>22</sup> lies within the limits of uncertainty imposed by the spectral resolution (Table S2, Supporting Information). However, unfortunately the signal-to-noise ratio of the present spectrum obtained from reduction of *cis*-Stb was such that it could not be confirmed whether the resonances identified as lying around 1.35 mT at lower or higher fields from the center of the spectrum were outermost resonances of the *cis*-Stb<sup>•-</sup> radical or whether there were resonances extending approximately 0.1 mT further out due to *trans*-Stb<sup>•-</sup>. Thus, in this sense, EPR spectroscopy of the electrolyzed solutions of *cis*-Stb was unable in its own right to provide totally unequivocal evidence of the *trans*-Stb radical anion. However, the fact that only one rather than two radical species appeared to be present after reduction of *cis*-Stb, combined with data derived from the present electrochemical studies and previous reports on the identity of the radical species formed from electrochemical or chemical reduction of stilbene isomers at room temperature,<sup>8,10–12,18,19</sup> leads to the

conclusion that the EPR spectrum derived from the electrolyzed *cis*-Stb solutions is due to the *trans*-isomer anion radical.

In summary, bulk electrolysis with voltammetric monitoring of the reaction and EPR spectroelectrochemical analysis confirmed the instability of the stilbene anion radicals, and also led to the conclusion that electrochemically induced isomerization of *cis*- to *trans*-Stb occurs after partial (ca. 50–60 mol %) electrolysis of the *cis*-isomer in CH<sub>3</sub>CN. Depletion of the radical anions produced by bulk electrolysis of *cis*-Stb proceeds presumably via reactions 3 (Scheme 1) and 5 with the formation of neutral stilbene molecules and electrochemically inactive bibenzyl.

**Influence of the (n-Bu)<sub>4</sub>NPF<sub>6</sub> Concentration on Voltammetric Reduction of *cis*-Stilbene in CH<sub>3</sub>CN.** Decreases in the magnitudes of the diffusion controlled limiting currents observed in near steady-state voltammetry for the reduction of *cis*-Stb in acetonitrile on increasing the concentration of the supporting electrolyte (Figure S1a, Supporting Information) can be attributed to increasing viscosity. However, more noteworthy is the effect related to changes in the half-wave potential ( $E_{1/2}$ ) for reduction (Figure 3).

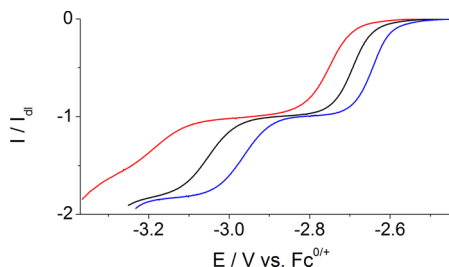


**Figure 3.** Near steady-state voltammograms obtained for reduction of 3.1 mM *cis*-stilbene in CH<sub>3</sub>CN containing 0.01 (blue), 0.10 (black), and 1.0 M (n-Bu)<sub>4</sub>NPF<sub>6</sub> (red) using a carbon fiber microelectrode at  $\nu = 0.005$  V s<sup>-1</sup>. Current data are normalized to that for the limiting current of the first reduction process.

In accordance with the results reported by Pletcher et al. for reduction of *trans*-Stb in dimethylformamide,<sup>26</sup> an increase in the concentration of (n-Bu)<sub>4</sub>NPF<sub>6</sub> in CH<sub>3</sub>CN shifts both *cis*-Stb reduction processes in CH<sub>3</sub>CN to more positive potentials, with the magnitude of the shift being larger for the second step (Figure 3). The supporting electrolyte concentration effect was rationalized by Pletcher et al.<sup>26</sup> in terms of ion pairing being more pronounced for the stilbene dianion as compared with the stilbene anion radical. Differences in concentration ratios used prevent direct comparison of the potential shifts with those reported by Pletcher et al.<sup>26</sup> for *trans*-Stb in dimethylformamide, but trends are similar. Half-wave potential ( $E_{1/2}$ ) data for the first and second reduction steps of *cis*-Stb versus the [Stb]/[(n-Bu)<sub>4</sub>NPF<sub>6</sub>] ratio are plotted in Figure 4. It would be expected that an increase in [Stb]/[(n-Bu)<sub>4</sub>NPF<sub>6</sub>] ratio should attenuate the effect of interaction of Stb<sup>•-</sup> and Stb<sup>2-</sup> with the tetrabutylammonium cation and shift  $E_{1/2}$  to more negative values closer to the “true” formal standard potentials of the Stb<sup>0/•-</sup> and Stb<sup>•-/2-</sup> processes.

ac Harmonics in the positive potential sweep of the FTAC cyclic voltammograms obtained from reduction of *cis*-Stb provide access to accurate values of  $E_{t0/t•-}^0$  (after correction using simulation for the influence of  $IR_u$  drop on the position of harmonic minima and maxima, which is particularly significant

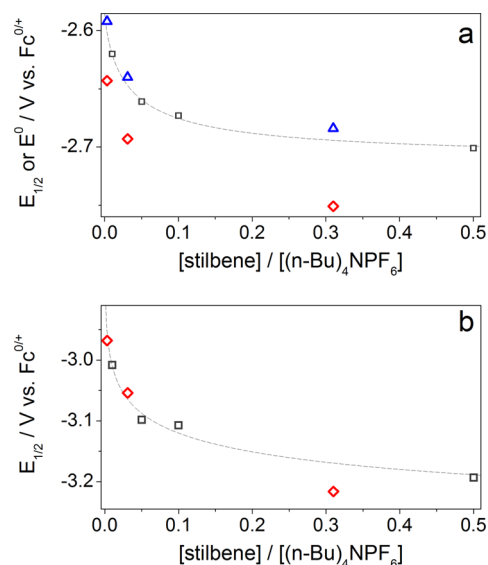


**Figure 4.** Influence of the [Stb]/[(n-Bu)<sub>4</sub>NPF<sub>6</sub>] ratio on potentials for the first (a) and second (b) stilbene reduction processes derived from voltammetric analysis of reduction of *cis*-Stb in CH<sub>3</sub>CN:  $E_{1/2}$  measured by near steady-state voltammetry (red  $\diamond$ );  $E^0$  for the *trans*-Stb<sup>0/•-</sup> process derived from FTAC voltammetric data (blue  $\triangle$ );  $E_{1/2}$  from steady-state voltammetry for reduction of *trans*-Stb in (CH<sub>3</sub>)<sub>2</sub>NCHO reported by Pletcher et al.<sup>26</sup> (black  $\square$ ). Dashed lines are guides to the eye.

with 0.01 M (n-Bu)<sub>4</sub>NPF<sub>6</sub> supporting electrolyte). This property was exploited to extract  $E_{t0/t•-}^0$  values from high-frequency (219 Hz) FTACV data obtained for reduction of *cis*-Stb in CH<sub>3</sub>CN at different concentrations of (n-Bu)<sub>4</sub>NPF<sub>6</sub>. Data in Figure 4a reveal that  $E_{t0/t•-}^0$  values obtained in this way agree well with  $E_{1/2}$  for the *trans*-Stb<sup>0/•-</sup> process in (CH<sub>3</sub>)<sub>2</sub>NCHO reported by Pletcher et al.,<sup>26</sup> particularly when uncertainties in reference potentials and other factors are taken into account. Thus, at similar [Stb]/[(n-Bu)<sub>4</sub>NPF<sub>6</sub>] ratios, the difference between  $E_{t0/t•-}^0$  in dimethylformamide and acetonitrile appears to be small.

$E_{1/2}$  values for the first *cis*-Stb reduction step are ca. 0.05–0.07 V more negative than those for *trans*-Stb<sup>0/•-</sup> (close to  $E^0$ ), and the difference ( $\Delta E_{1/2}$ ) is slightly affected by the [Stb]/[(n-Bu)<sub>4</sub>NPF<sub>6</sub>] ratio (Figure 4a). The  $\Delta E_{1/2}$  values conform acceptably to published differences in  $E^0$  for the *cis*-Stb<sup>0/•-</sup> and *trans*-Stb<sup>0/•-</sup> processes (see ref 2 and references therein).  $E_{1/2}$  for the second *cis*-Stb reduction step at low [Stb]/[(n-Bu)<sub>4</sub>NPF<sub>6</sub>] ratios in CH<sub>3</sub>CN conform well to those reported by Pletcher et al.<sup>26</sup> for the second reduction step of *trans*-Stb except for the lowest concentration of (n-Bu)<sub>4</sub>NPF<sub>6</sub>.

Increasing the concentration of (n-Bu)<sub>4</sub>NPF<sub>6</sub> in CH<sub>3</sub>CN solution of *cis*-Stb does not cause any noteworthy changes in the characteristics of the transient dc cyclic voltammograms except those arising from differences in  $R_u$  (Figure 5 and Figure S6, Supporting Information).

In particular, the complete chemical irreversibility of the second *cis*-Stb reduction step is retained at all [*cis*-Stb]/[(n-Bu)<sub>4</sub>NPF<sub>6</sub>] ratios examined (Figure 5b and Figure S6b, Supporting Information). This interpretation is in contrast to that of Pletcher et al.<sup>26</sup> who suggested, on the basis of their near steady-state voltammetry data, that the reversibility of the Stb<sup>•-/2-</sup> process improves at high concentrations of (n-Bu)<sub>4</sub>NPF<sub>6</sub> in (CH<sub>3</sub>)<sub>2</sub>NCHO. Nevertheless, it is clear that ion

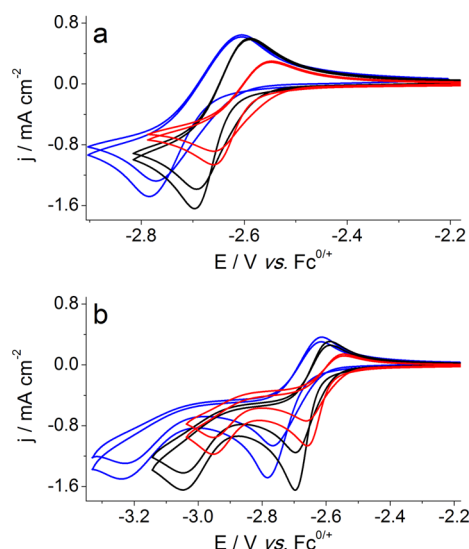


**Figure 5.** dc Cyclic voltammograms ( $\nu = 0.10 \text{ V s}^{-1}$ ) for (a) the first and (b) both steps of reduction of 3.1 mM *cis*-stilbene (the first two cycles of potential are shown) with a Au electrode in  $\text{CH}_3\text{CN}$  containing 0.01 (blue), 0.10 (black), and 1.0 M (*n*-Bu) $_4\text{NPF}_6$  (red).

pairing provided by the supporting electrolyte is significant in a molecular solvent.

**Cyclic Voltammetry of *cis*-Stilbene in ILs.** Ionic liquids provide a very high ionic strength environment where ion pairing can be extremely significant, and hence can stabilize anion radicals and dianions generated by reduction of conjugated olefins. The media of interest in this study are also highly aprotic which could prevent protonation of the stilbene dianion found in  $\text{CH}_3\text{CN}$  even at very high stilbene concentration.<sup>22</sup> To observe chemical reversibility (equal reduction and oxidation peak currents) for the second *cis*-Stb reduction step, cyclic voltammetric measurements have to be undertaken on concentrated ( $\geq 0.1 \text{ M}$ ) *cis*-Stb solutions in the aprotic ionic liquids Pyr $_{1,4}$ -NTf $_2$  (Figure 6) and (N $_{111}$ )(N $_{112}$ )-BH $_2$ -NTf $_2$  (Figure S7, Supporting Information). That is, in accordance with previous findings on reduction of *trans*-Stb,<sup>22</sup> direct observation of dianions only became possible on the time scale of cyclic voltammetry at room temperature when the stilbene concentration in bulk solution significantly exceeds that of adventitious water and other proton-donating impurities present in the ILs even after extensive purification (cf. Figure 6a and Figure S8, Supporting Information).

Under these high stilbene concentration conditions, a distinction in cyclic voltammograms is found for reduction of *cis*- and *trans*-stilbenes in Pyr $_{1,4}$ -NTf $_2$  in the initial short “induction period” only (see inset in Figure 6a). This difference mimics observations made in  $\text{CH}_3\text{CN}$ . The significant  $I_{\text{R}_u}$  drop that broadens the response may mask other subtle differences. Importantly, the chemically reversible dc response found in the second cycle of potential for *cis*-Stb is experimentally indistinguishable from that reported for the *trans*-isomer in the pyrrolidinium-based IL. Clearly, electrochemically induced *cis* to *trans* isomerization also occurs in this IL. Even at a similarly high concentration of *cis*-Stb in (N $_{111}$ )(N $_{112}$ )BH $_2$ -NTf $_2$ , the again chemically reversible Stb $^{\bullet-}/2-$  process is preceded by an irreversible reduction process (Figure S7, Supporting Information), presumably associated with formation of the protonated dianion arising from a higher

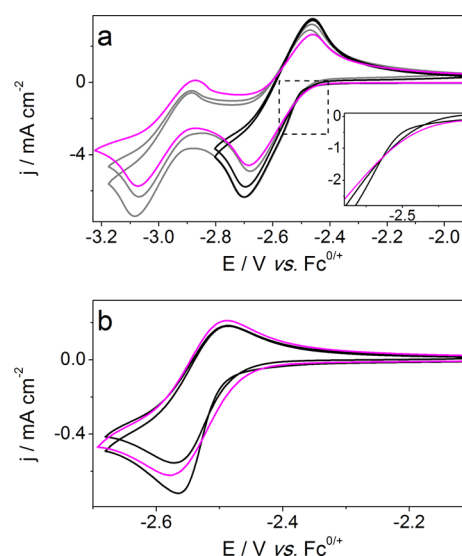


**Figure 6.** dc Cyclic voltammograms ( $\nu = 0.10 \text{ V s}^{-1}$ ) obtained at (a) high (0.15 M) and (b) low (0.01 M) concentrations for reduction of *cis*- (black and gray, the first two cycles of potential are shown) and *trans*-stilbene (magenta) in Pyr $_{1,4}$ -NTf $_2$  with (a) GC and (b) Au electrodes. The inset in part (a) represents an expanded version of the region of the voltammogram outlined in the main plot for the black and magenta data.

concentration of water or other proton-donating impurities present in this IL as compared to Pyr $_{1,4}$ -NTf $_2$ .<sup>22</sup>

The first process is readily studied at low stilbene concentrations in the ionic liquids. dc Cyclic voltammetric reduction of 10 mM *cis*-Stb in Pyr $_{1,4}$ -NTf $_2$  (Figure 6b) proceeds in a qualitatively similar manner to that found in acetonitrile containing (*n*-Bu) $_4\text{NPF}_6$  as the supporting electrolyte (Figures 1 and 5). However, in the pyrrolidinium-based IL, the *cis*-Stb $^{0/\bullet-}$  and *trans*-Stb $^{0/\bullet-}$  processes provide only a very small ca. 0.005–0.008 V difference between the minima of even harmonics registered in the first negative potential (reductive) sweep of the FTAC voltammograms for 10 mM *cis*- and *trans*-Stb (Figure 7). This small difference detected in high frequency FTACV data can be compared to that of ca. 0.03–0.04 V found for reduction of the stilbene isomers in  $\text{CH}_3\text{CN}$ . ac voltammetric responses for 10 mM *cis*-Stb in the reverse (positive) scan direction and all subsequent cycles in Pyr $_{1,4}$ -NTf $_2$  closely resemble those obtained in all cycles for the reduction of *trans*-Stb (Figure 7). These observations suggest that substantial isomerization of *cis*-Stb to the *trans*-counterpart occurs at more positive potentials (with respect to  $E^0$  of *trans*-Stb $^{0/\bullet-}$ ), or that the difference between  $E^0$  for the *trans*-Stb $^{0/\bullet-}$  and *cis*-Stb $^{0/\bullet-}$  processes is less in Pyr $_{1,4}$ -NTf $_2$  than in  $\text{CH}_3\text{CN}$ .

Reversible potentials for electroreduction of *cis*- and *trans*-stilbene in Pyr $_{1,4}$ -NTf $_2$  are less negative than those found in  $\text{CH}_3\text{CN}$  in the presence of 1.0 M (*n*-Bu) $_4\text{NPF}_6$  by at least 0.04 V. This may be indicative of either an enhanced ion pairing effect provided by a high concentration of Pyr $_{1,4}^+$  cations in IL or medium dependence of  $E^0$  for the Fc $^{0/+}$  reversible potential.

**Simulations of dc and ac Voltammetry for Reduction of *cis*-Stilbene.** The data derived from voltammetric studies, bulk electrolysis, and EPR experiments provide persuasive evidence for the occurrence of fast isomerization of *cis*-stilbene to the *trans*-counterpart upon acceptance of one electron. In principle, this could be the result of a single isomerization step



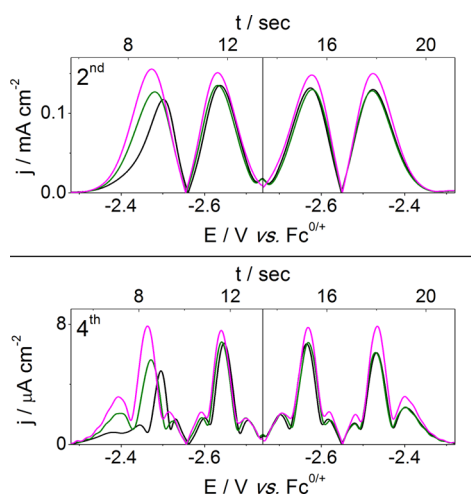


**Figure 7.** Second and fourth ac harmonic components of FTAC cyclic voltammograms obtained for reduction of 10 mM *cis*-stilbene during the first two cycles of dc potential (black, first; green, second) and 10 mM *trans*-stilbene (magenta) in Pyr<sub>14</sub>–NTf<sub>2</sub> with a Au electrode.  $f = 219$  Hz,  $\Delta E = 0.08$  V,  $\nu = 0.060$  V s<sup>−1</sup>. The time scale corresponds to the black data.

via reaction 1 with involvement of the cross redox reaction 4 (Scheme 1). However, numerous attempts to match the experimental voltammetric data for reduction of *cis*-Stb with simulations based on this mechanism were all unsuccessful. On the basis of the literature data reported in the Introduction, the most likely reaction scheme is the complete mechanism given in Scheme 1 with negligible influence of the *cis*-Stb<sup>•−</sup> ⇌ *trans*-Stb<sup>•−</sup> process. Simulations of this mechanism with inclusion of all possible cross redox reactions can generate dc and ac voltammograms that acceptably agree with the experimental data obtained in CH<sub>3</sub>CN (0.1 M (*n*-Bu)<sub>4</sub>NPF<sub>6</sub>) (Figures 8 and 9, simulation parameters are listed in Table S3, Supporting Information) when the following assumptions are adopted:

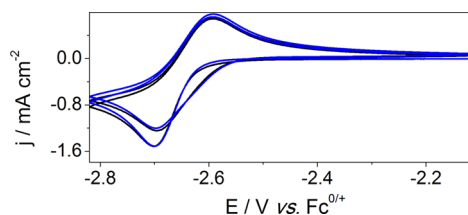


**Figure 8.** Comparison of experimental dc cyclic voltammograms ( $\nu = 0.10$  V s<sup>−1</sup>; first two cycles) for reduction of 3.1 mM *cis*-stilbene with a GC electrode in CH<sub>3</sub>CN (0.1 M (*n*-Bu)<sub>4</sub>NPF<sub>6</sub>) (black) and simulated curve (blue). The simulation is based on the mechanism in Scheme 1 (neglecting reaction 1) coupled to all possible cross redox reactions between the Stb<sup>0</sup>, Stb<sup>•−</sup>, and Stb<sup>2−</sup> species and use of the parameters listed in Table S3 (Supporting Information).

(a) The diffusion coefficient of *cis*-Stb<sup>0</sup> ( $D_{c0}$ ) is  $2.5 \times 10^{-5}$  cm<sup>2</sup> s<sup>−1</sup>, as derived from the microelectrode diffusion limited current obtained versus the reference data for oxidation of Fc internal standard with  $D_{Fc} = 2.4 \times 10^{-5}$  cm<sup>2</sup> s<sup>−1</sup> (Figure S1a, Supporting Information).<sup>27</sup> The diffusion coefficients of *cis*-Stb<sup>•−</sup> and *cis*-Stb<sup>2−</sup> are then estimated to be  $0.85 \cdot D_{c0} = 2.1 \times 10^{-5}$  cm<sup>2</sup> s<sup>−1</sup> on the basis of the relationship of the  $D$  values established for *trans*-Stb<sup>0</sup> and *trans*-Stb<sup>•−</sup>.<sup>28</sup>

(b) Charge transfer coefficients of all electron transfer steps are equal to 0.50.

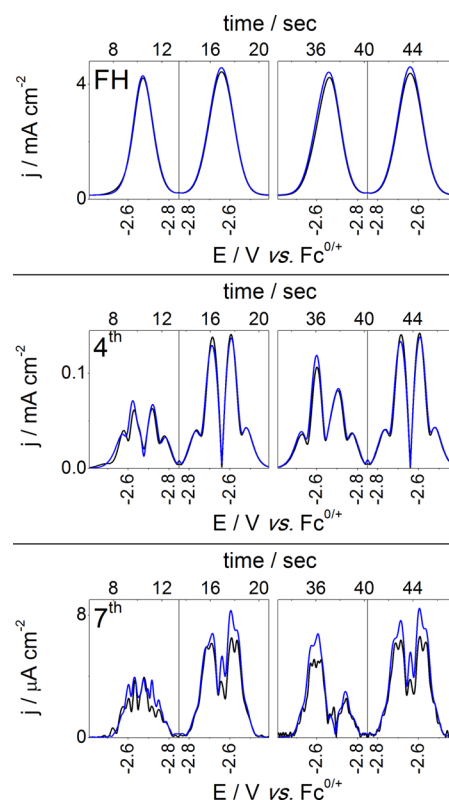


**Figure 9.** Fundamental, fourth, and seventh ac harmonic components of FTAC cyclic voltammograms obtained with a GC electrode for reduction of 3.1 mM *cis*-stilbene (black; panels on the left- and right-hand sides show the first and second cycles of dc potential, respectively) in CH<sub>3</sub>CN (0.1 M (*n*-Bu)<sub>4</sub>NPF<sub>6</sub>) and simulated data (blue). Experimental parameters:  $f = 9$  Hz;  $\Delta E = 0.08$  V;  $\nu = 0.060$  V s<sup>−1</sup>;  $R_u = 72$  Ω;  $C_{DL} = 32$  μF cm<sup>−2</sup>. Simulation parameters are as in Figure 8.

(c) The same  $E^0$  and  $k^0$  for the *trans*-Stb<sup>0/•−</sup> and *trans*-Stb<sup>•−/2−</sup> processes as well as the rate constant for the irreversible protonation of *trans*-Stb<sup>2−</sup> (under the assumption of a pseudo-first-order reaction with respect to the dianion) (reaction 3t in Scheme 1) apply, as reported in low (9 Hz) and high frequency (219 Hz) ac voltammetric studies for reduction of *trans*-Stb.<sup>22</sup>

(d) *cis*-Stb<sup>0/•−</sup> and *cis*-Stb<sup>•−/2−</sup> processes are fast on the time scale of the voltammetric experiment.

(e)  $E^0$  for the *cis*-Stb<sup>0/•−</sup> process is equal to or more negative (within a 0.10 V range) than that for the *trans*-Stb<sup>0/•−</sup> couple, as follows from the experimental voltammetric data.  $E^0$  for the *cis*-Stb<sup>•−/2−</sup> process is equal to or more positive (within a 0.10 V range) than that for the *trans*-Stb<sup>•−/2−</sup> process, as suggested by Combéllas et al.<sup>2</sup>

(f) The rate constant for the protonation step in reaction 3c is similar to that of reaction 3t (Scheme 1).

(g) The isomerization step *cis*-Stb<sup>•−</sup> ⇌ *trans*-Stb<sup>•−</sup> does not occur on the time scale of the voltammetric experiment.

(h) The equilibrium constants of the cross redox reactions between the Stb<sup>0</sup>, Stb<sup>•−</sup>, and Stb<sup>2−</sup> species are calculated in accordance with the chosen  $E^0$  values, and the highest rate constant for all of these processes lies at the diffusion controlled limit ( $10^{10}$  M<sup>−1</sup> s<sup>−1</sup>).

(i) An additional homogeneous chemical process for depletion of *cis*-stilbene radical anions is introduced. A plausible chemical transformation of the *cis*-stilbene radical anions would

be irreversible dimerization to give a dianion:  $2\text{cis-Stb}^{\bullet-} \rightarrow [\text{Stb}]_2^{2-}$  (6), which, in turn, may be rapidly protonated to produce 1,2,3,4-tetraphenylbutane.<sup>29</sup> The slight inequality of limiting current magnitudes of the two reduction steps derived from the near steady-state voltammetry (Figure S1, Supporting Information, and Figure 3) also required an additional chemical transformation of this kind. In the absence of this step, current magnitudes do not match experimental data as well as when it is included. As described elsewhere,<sup>22</sup> successful simulation of both dc and ac voltammetric data for reduction of *trans*-Stb under similar conditions can be achieved without inclusion of a homogeneous chemical process for depletion of *trans*-Stb<sup>•−</sup>.

(j) The effect of ion pairing is neglected.

Even with this mechanism, an ideal fit was not achieved, as evidenced by small differences in experimental and simulated higher ac harmonics data (seventh harmonic in Figure 9). Obviously, the parameters listed in Table S3 (Supporting Information) do not necessarily provide the best possible simulation available and, probably, better agreement between the experiment and simulations could be acquired. However, there are too many adjustable parameters to make this exercise useful in a meaningful manner. Furthermore, it should be noted that the simulations of dc and ac voltammetric data are not very sensitive to certain parameters; for example, use of any  $k^0$  value above  $0.10 \text{ cm s}^{-1}$  does not make a significant difference. Therefore, finding via heuristic means a unique set of parameters allowing a “perfect” fit of both dc and ac voltammetric experimental data with the considered mechanism or related ones appears to be problematic. Nevertheless, it is noted that the basic features of ac and dc voltammograms for reduction of *cis*-Stb (including the nonzero intercept at  $\nu = 0$  of the  $I_p^{\text{Red}} - \nu^{1/2}$  dependence derived from the first cycle (Figure S2, Supporting Information)) are acceptably mimicked by the simulations presented (Figures 8 and 9).

FTAC voltammetric studies of the reduction of *cis*-Stb at concentrations above 0.1 M in the  $\text{Pyr}_{1,4}\text{-NTf}_2$  and  $(\text{N}_{111})\text{-(N}_{112})\text{BH}_2\text{-NTf}_2$  ionic liquids are not readily tractable due to the very large  $IR_u$  drop associated with large magnitudes of both the current ( $I$ ) and uncompensated resistance ( $R_u$ ), the former being associated with high concentration and the latter being due to the moderate conductivities of these ILs. Simulations of the FTAC voltammetric data for reduction of 10 mM *cis*-Stb in  $\text{Pyr}_{1,4}\text{-NTf}_2$  were not undertaken in detail due to the lack of knowledge on the parameters associated with the increased complexity of the second reduction step which proceeds in two stages under these lower concentration conditions (Figure S8, Supporting Information). However, fast electrochemically induced isomerization is again evident and the basic features of the isomerization appear to be the same as in  $\text{CH}_3\text{CN}$ . Simulations of the cyclic voltammograms obtained for reduction of 10 mM *trans*-Stb in  $\text{Pyr}_{1,4}\text{-NTf}_2$  under the assumption that the *trans*-Stb<sup>0/•−</sup> process is uninfluenced by the second reduction step imply that  $k_{0/t,\bullet-}^0$  at a Au electrode in this IL is  $0.02\text{--}0.04 \text{ cm s}^{-1}$ . This is an order of magnitude smaller than the value found in  $\text{CH}_3\text{CN}$  (0.1 M  $(n\text{-Bu})_4\text{NPF}_6$ ). However, this process is close to the reversible limit and considerable uncertainty exists in the provided  $k_{0/t,\bullet-}^0$  value.

## CONCLUSIONS

The effect of medium on the electrochemically induced isomerization of *cis*-Stb has been studied in the molecular solvent acetonitrile containing  $(n\text{-Bu})_4\text{NPF}_6$  as the supporting electrolyte and in the highly aprotic ionic liquids  $\text{Pyr}_{1,4}\text{-NTf}_2$

and  $(\text{N}_{111})(\text{N}_{112})\text{BH}_2\text{-NTf}_2$ . In agreement with the results reported by Pletcher et al.<sup>26</sup> for electroreduction of *trans*-Stb in dimethylformamide, the  $E_{1/2}$  value for the *cis*-Stb<sup>0/•−/2−</sup> processes and  $E^0$  for *trans*-Stb<sup>0/•−</sup> in acetonitrile are found to shift to more positive values upon increasing the  $[\text{Stb}]/[(n\text{-Bu})_4\text{NPF}_6]$  ratio. However, within the  $(n\text{-Bu})_4\text{NPF}_6$  concentration range examined (0.01–1.0 M) and with 1–5 mM *cis*-Stb, complete chemical irreversibility of the second stilbene reduction step is retained as is extensive *cis*–*trans* isomerization detected voltammetrically irrespective of the  $[\text{Stb}]/[(n\text{-Bu})_4\text{NPF}_6]$  ratio. Heuristic comparisons of experimental voltammetric data for reduction of *cis*-Stb with simulation data do not allow unambiguous ascertainment of the mechanism of the electrochemically induced isomerization at room temperature in  $\text{CH}_3\text{CN}$  with  $(n\text{-Bu})_4\text{NPF}_6$  as the supporting electrolyte. Nevertheless, a reaction scheme based on the disproportionation of *cis*-stilbene radical anions and fast transformation of the *cis*-dianion to the *trans*-configuration appears plausible and is in accordance with the conclusions of Szwarc et al.<sup>12,17,18,20</sup> made on the basis of the kinetic analysis of the chemical reduction of *cis*-Stb. Differences in potentials for the *cis*-Stb<sup>0/•−</sup> and *trans*-Stb<sup>0/•−</sup> reduction processes are found to be less pronounced in the  $\text{Pyr}_{1,4}\text{-NTf}_2$  ionic liquid than in the molecular solvent acetonitrile. The data obtained provide another example of the substantial influence of the medium on the characteristics of electron-transfer processes.

## ASSOCIATED CONTENT

### Supporting Information

Experimental details for electrochemical, NMR, and EPR measurements. Figure S1 shows near steady-state voltammograms for reduction of *cis*-stilbene. Figure S2 shows Randles–Sevcik dependencies for reduction of *cis*-stilbene. Table S1 contains  $\Delta E_p$  data for dc cyclic voltammetric reduction of *cis*- and *trans*-stilbene. Figure S3 shows dc voltammograms for reduction of *cis*-stilbene and *cis*-4-methoxystilbene in  $\text{CH}_3\text{CN}$ . Figure S4 shows FTACV data for electrolyzed *cis*-stilbene solution. Figure S5 shows EPR spectra generated from reduction of *cis*- and *trans*-stilbene in  $\text{CH}_3\text{CN}$ . Table S2 reports  $g$ -values and line widths of EPR spectra obtained from reduction of  $\text{CH}_3\text{CN}$  solutions of *cis*- and *trans*-stilbene. Figure S6 compares scaled dc voltammograms for reduction of *cis*-stilbene in 0.1 and 1.0 M  $(n\text{-Bu})_4\text{NPF}_6$  acetonitrile solutions. Figure S7 shows dc voltammograms for reduction of *cis*-stilbene and *cis*-4-methoxystilbene in  $(\text{N}_{111})(\text{N}_{112})\text{BH}_2\text{-NTf}_2$ . Figure S8 shows dc voltammograms for reduction of *cis*-stilbene in  $\text{Pyr}_{1,4}\text{-NTf}_2$ . Table S3 reports parameters used in voltammetric simulations. This material is available free of charge via the Internet at <http://pubs.acs.org>.

## AUTHOR INFORMATION

### Corresponding Authors

\*E-mail: Alexandr.Simonov@monash.edu.

\*E-mail: Alan.Bond@monash.edu.

### Present Address

<sup>†</sup>Faculty of Science, Taibah University, Madinah, Saudi Arabia.

### Notes

The authors declare no competing financial interest.

## ACKNOWLEDGMENTS

The authors are grateful to the Frontier Scientific company ([www.frontiersci.com](http://www.frontiersci.com), Logan, UT, USA) for a generous



donation of  $(N_{111})(N_{112})BH_2-NTf_2$  ionic liquid. The Monash University authors acknowledge financial support from the Australian Research Council under Discovery Project No. 120101470.

## REFERENCES

- (1) Pombeiro, A. J. L.; da Silva, M. F. C. G.; Lemos, M. A. N. D. A. Electron-transfer Induced Isomerizations of Coordination Compounds. *Coord. Chem. Rev.* **2001**, 219–221, 53–80.
- (2) Combellas, C.; Kanoufi, F.; Stoytcheva, M.; Thiébaud, A. Cation Effects in the Reduction of Stilbenes in Liquid Ammonia. *J. Phys. Chem. B* **2004**, 108, 2756–2763.
- (3) Kraiya, C.; Singh, P.; Todres, Z. V.; Evans, D. H. Voltammetric Studies of the Reduction of cis- and trans- $\alpha$ -Nitrostilbene. *J. Electroanal. Chem.* **2004**, 563, 171–180.
- (4) Waskiewicz, K.; Gabanski, R.; Motyka, R.; Lapkowski, M.; Suwinski, J.; Zak, J. Photochemical and Electrochemical Z–E Isomerization of 1,4-Dialkoxy-2,5-bis[2-(thien-2-yl)ethenyl]benzene Stereoisomers. *J. Electroanal. Chem.* **2008**, 617, 27–37.
- (5) Chen, Y.-C.; Sun, W.-T.; Lu, H.-F.; Chao, I.; Huang, G.-J.; Lin, Y.-C.; Huang, S.-L.; Huang, H.-H.; Lin, Y.-D.; Yang, J.-S. A Pentiptycene-Derived Molecular Brake: Photochemical E→Z and Electrochemical Z→E Switching of an Enone Module. *Chem.—Eur. J.* **2011**, 17, 1193–1200.
- (6) Hoijsink, G. J.; van der Meij, P. H. Mono- and Di-negative Ions of 1, n-Diphenylpolyenes and Tetraphenylcumulenes. *Z. Phys. Chem.* **1959**, 20, 1–14.
- (7) Waack, R.; Doran, M. A. Radical-anions of Olefins; a Mechanism for Geometric Isomerization. *J. Organomet. Chem.* **1965**, 3, 94–96.
- (8) Bard, A. J.; Puglishi, V. J.; Kenkel, J. V.; Lomax, A. Reductive Coupling and Isomerization of Electrogenated Radical Ions of cis- and trans-Isomers. *Faraday Discuss. Chem. Soc.* **1973**, 56, 353–366.
- (9) Chang, R.; Markgraf, J. H. ESR and UV Study of an Electron Transfer Reaction. *Chem. Phys. Lett.* **1972**, 13, 575–576.
- (10) Chang, R.; Johnson, C. S. ESR Spectrum and Barrier to Internal Rotation for the Stilbene Anion Radical. *J. Chem. Phys.* **1964**, 41, 3272–3274.
- (11) Takahashi, C.; Maeda, S. Raman Spectra of Stilbene Negative Ions in Tetrahydrofuran Solution. *Chem. Phys. Lett.* **1974**, 28, 22–26.
- (12) Sorensen, S.; Levin, G.; Szwarc, M. Electron-Transfer Induced Isomerization of cis-Stilbene in Hexamethylphosphoramide. Isomerization Mediated by the Free Ions of Stilbenides Radicals. *J. Am. Chem. Soc.* **1975**, 97, 2341–2345.
- (13) Dietz, R.; Peover, M. E. Stereochemical Effects in the Electrochemistry of some Hindered Stilbenes in Dimethylformamide. *Discuss. Faraday Soc.* **1968**, 45, 154–166.
- (14) Levin, G.; Ward, T. A.; Szwarc, M. Electron-Transfer Catalyzed Cis-Trans Isomerization of Stilbene. The Stability of Sodium cis-Stilbenide and the Existence of Sodium Salts of cis- and of trans-Stilbene Dianions. *J. Am. Chem. Soc.* **1974**, 96, 270–272.
- (15) Jensen, B. S.; Lines, R.; Pagsberg, P.; Parker, V. D. The Configuration Stability of Stilbene Anion Radicals. *Acta Chem. Scand., Ser. B* **1977**, 31, 707–710.
- (16) Levanon, H.; Neta, P. Electron Transfer, Equilibrium, and Protonation in the System of cis- and trans-Stilbene in 2-Propanol. *Chem. Phys. Lett.* **1977**, 48, 345–349.
- (17) Wang, H. C.; Levin, G.; Szwarc, M. Kinetics of Isomerization of the Free cis-Stilbene Radical Anion into Its Trans Isomer in Hexamethylphosphoric Triamide. Spectroscopic and Electron Spin Resonance Identification of cis-Stilbene Radical Anion in Tetrahydrofuran. *J. Am. Chem. Soc.* **1977**, 99, 2642–2647.
- (18) Gerson, F.; Ohya-Nishiguchi, H.; Szwarc, M.; Levin, G. The ESR Spectrum of the cis-Stilbene Radical Anion. *Chem. Phys. Lett.* **1977**, 52, 587–589.
- (19) Nozaki, K.; Naito, A.; Ho, T.-I.; Hatano, H.; Okazaki, S. Kinetic Studies of Cis-Trans Isomerization of Stilbene Anion Radicals with a Quantitative-Electrolysis ESR Method. *J. Phys. Chem.* **1989**, 93, 8304–8309.
- (20) Ward, T. A.; Levin, G.; Szwarc, M. Electron Transfer Induced Cis-Trans Isomerization of Stilbene. The Effect of Counterions and the Existence of Two Isomeric Stilbene Dianions. *J. Am. Chem. Soc.* **1975**, 96, 258–261.
- (21) Bond, A. M.; Duffy, N. W.; Guo, S.-X.; Zhang, J.; Elton, D. Changing the Look of Voltammetry. Can FT revolutionize voltammetric techniques as it did for NMR? *Anal. Chem.* **2005**, 77, 186A–195A.
- (22) Abdul-Rahim, O.; Simonov, A. N.; Rüther, T.; Boas, J. F.; Torriero, A. A. J.; Collins, D. J.; Perlmutter, P.; Bond, A. M. The Observation of Dianions Generated by Electrochemical Reduction of trans-Stilbenes in Ionic Liquids at Room Temperature. *Anal. Chem.* **2013**, 85, 6113–6120.
- (23) <http://www.elchsoft.com>.
- (24) <http://www.garethkennedy.net/MECSim.html>.
- (25) *Organic Chemistry*, 3rd ed.; Chalice, J., Ed.; Prentice Hall International, Inc.: University of California, Santa Barbara, CA, 2001; p 637.
- (26) Geraldo, M. D.; Montenegro, M. I.; Slevin, L.; Pletcher, D. A. Microelectrode Study of the Reduction of Phenyl-Substituted Ethenes in Toluene/Dimethylformamide Mixtures. *J. Phys. Chem. B* **2001**, 105, 3182–3186.
- (27) Janisch, J.; Ruff, A.; Speiser, B.; Wolff, C.; Zigelli, J.; Benthin, S.; Feldmann, V.; Mayer, H. A. Consistent Diffusion Coefficients of Ferrocene in Some Non-aqueous Solvents: Electrochemical Simultaneous Determination Together with Electrode Sizes and Comparison to Pulse-gradient Spin-echo NMR Results. *J. Solid State Electrochem.* **2011**, 15, 2083–2094 and references therein.
- (28) Pedersen, S. U.; Christensen, T. B.; Thomasen, T.; Daasbjerg, K. New Methods for the Accurate Determination of Extinction and Diffusion Coefficients of Aromatic and Heteroaromatic Radical Anions in N,N-Dimethylformamide. *J. Electroanal. Chem.* **1998**, 454, 123–143.
- (29) Wawzonek, S.; Blaha, E. W.; Berkey, R.; Runner, M. E. Polarographic Studies in Acetonitrile and Dimethyl-formamide. II. Behavior of Aromatic Olefins and Hydrocarbons. *J. Electrochem. Soc.* **1955**, 102, 235–242.